View metadata, citation and similar papers at core.ac.uk

brought to you by CORE

provided by University of Bath Research Portal

Citation for published version:
Milewski, PA & Wang, Z 2013, 'Three dimensional flexural–gravity waves', Studies in Applied Mathematics, vol. 131, no. 2, pp. 135-148. https://doi.org/10.1111/sapm.12005

DOI:
10.1111/sapm.12005

Publication date:
2013

Document Version
Peer reviewed version

Link to publication

University of Bath

General rights
Copyright and moral rights for the publications made accessible in the public portal are retained by the authors and/or other copyright owners and it is a condition of accessing publications that users recognise and abide by the legal requirements associated with these rights.

Take down policy
If you believe that this document breaches copyright please contact us providing details, and we will remove access to the work immediately and investigate your claim.

Download date: 13. May. 2019

Three Dimensional Flexural–Gravity Waves

By P. A. Milewski and Z. Wang

Waves propagating on the surface of a three–dimensional ideal fluid of arbitrary depth bounded above by an elastic sheet that resists flexing are considered in the small amplitude modulational asymptotic limit. A Benney–Roskes–Davey–Stewartson model is derived, and we find that fully localized wavepacket solitary waves (or lumps) may bifurcate from the trivial state at the minimum of the phase speed of the problem for a range of depths. Results using a linear and two nonlinear elastic models are compared. The stability of these solitary wave solutions and the application of the BRDS equation to unsteady wave packets is also considered. The results presented may have applications to the dynamics of continuous ice sheets and their breakup.

1. Introduction

In this work we consider the problem of waves on the surface of an incompressible inviscid fluid in three–dimensions bounded above by a flexible elastic sheet and below by a horizontal bottom. The two restoring forces are gravity acting on the fluid and the resistance to flexural bending of the sheet. Three simple elasticity models appropriate for thin flexible sheets will be compared. Two of the models, the linear Euler–Bernoulli model used in several studies [1], [2] and a Cosserat–type nonlinear model used in [3], can be written in terms of their contribution to the total Hamiltonian of the problem:

$$\mathbb{H}_L = D\frac{1}{2}\int (\Delta\eta)^2 \, dA, \qquad \mathbb{H}_C = D\frac{1}{2}\int (\kappa_1+\kappa_2)^2 \, dS, \tag{1}$$

Address for correspondence: P.A. Milewski, Department of Mathematical Sciences, University of Bath, Bath, BA2 7AY, UK; e-mail: p.a.milewski@bath.ac.uk

DOI: 10.1111/sapm.12005

STUDIES IN APPLIED MATHEMATICS 00:1–14
© 2013 by the Massachusetts Institute of Technology

where D is the constant bending modulus or flexural rigidity of the sheet, κ_1, κ_2 are its principal curvatures, η is the sheet displacement, Δ is the horizontal Laplacian, and dA and dS are the horizontal and surface area elements, respectively. These elasticity models yield a restoring force in the form of a pressure jump across the elastic sheet given by the variational derivative $\frac{\delta \mathbb{H}}{\delta \eta}$ which, for the linear model, this is given by the biharmonic $D\Delta^2\eta$. The third model which has been extensively used (see [4]) is the Kirchoff–Love (KL) model, whereby the pressure jump for a one–dimensional free surface is expressed directly as $D\partial_x^2\kappa$, where κ is the curvature. This model does not appear to have a Hamiltonian or conservative formulation. The principal approximations common to all the models are that the sheet is thin, and that its inertia and its stretching are neglected [1].

Flexural Gravity (FG) models have been used to study free and forced waves propagating on a continuous ice sheet floating over water. A thorough treatment of the linear problem under various modeling assumptions together with a review of experimental work is found in the book in [2]. An interesting particular case is that of near–critical forcing which occurs when a load moves at a speed close to the minimum phase speed of linear waves (see below). In that case the free surface displacement can be large and nonlinear effects may be important since at criticality, linear nondissipative theories predict a displacement that grows unbounded with time. The nonlinear resolution of this issue inspired the work in [4] on the steady forced nonlinear response. They studied the two–dimensional fluid problem using a KL nonlinear elasticity model and performed a normal–form weakly nonlinear analysis near the phase speed minimum. Their analysis includes the derivation of modulation equations, in this case a one–dimensional Nonlinear Schrödinger (NLS) equations, which is defocussing (Benjamin–Feir stable) in infinite depth and focussing for water shallower than a critical depth. The latter allows for solitary waves. The situation *at this critical wave speed* is opposite to pure gravity waves which are Benjamin–Feir stable in shallower water. Free solitary waves play an important role in understanding the critically forced transient response, which in this case was studied using fully nonlinear unsteady computations in [5].

Nonlinear computations and weakly nonlinear analysis of free periodic and solitary waves in the FG problem have been performed by several authors using the three principal elasticity models above. Note that, even if the elasticity model is linear, the fluid equations bring nonlinearity into the problem and that both nonlinear elasticity models yield the linear elastic model in the limit of small amplitude waves. Two–dimensional Stokes waves were first considered in [6] using a KL model. Fully nonlinear periodic, solitary, and generalized solitary waves to the KL model were considered in [4], [5], and [7], and solitary waves in the Cosserat model were considered in [8]. In three–dimensions, to our knowledge, only the linear model has been used to study structures which are solitary in the propagation direction and transversally periodic

in [9], and similar solutions in shallow water in [10] from a small amplitude KP–type model. In [11], the work most closely related to the present, a Benney–Roskes–Davey–Stewartson (BRDS) equation in the *shallow* water regime was shown to support Dromions. These are structures whose surface deflection is localized but whose mean flow component has support on an unbounded "X–shaped" region in the plane.

Regarding sea–ice applications, [12] derived a one–dimensional NLS equation for modulations of FG waves with the assumption of precompressed ice state. In that paper they also propose an explanation for a large amplitude waves in the Weddell Sea, although the modeling assumption of a continuous ice sheet may be too idealized. Here, we show that the modulation equations for fully two dimensional waves is far richer and may include violent focussing in finite depth. Continuous semi–infinite ice sheets are often used as a model for the transmission and reflection of ocean waves onto the ice [1]. The present modulation theory may be valid for the subsequent evolution of these wave on the ice sheet.

In this paper, we generalize the weakly nonlinear modulational analysis of this problem to three–dimensions and arbitrary depth. The corresponding wave–packet equations are the BRDS system ([13] and [14]) whose type will vary with the physical parameters of the problem and the elastic model. We then consider waves in two regimes. First, we discuss in detail the special case with carrier wavenumber equal to that of the *minimum* of the dispersion relation. These are waves likely to be generated at almost critical forcing speeds. At phase speed minima, the phase and group speeds are equal and hence solitary waves of the BRDS system will correspond to traveling solitary waves of the primitive equations. We give conditions on water depth for the existence of these waves and compute their envelope profiles. A similar BRDS–type analysis for the related problem of capillary–gravity waves was considered in [15], but there are substantial differences in the solutions. Second, we also discuss the consequences of the resulting BRDS system for wave packets whose carrier wave is not near the phase–speed minimum. The resulting unsteady evolution is applicable to the general problem of modulated FG wave propagation.

The phase speed relation for the linearized FG model is given by

$$c^2 = \tanh\left(|k|H\right)\left(\frac{1}{|k|} + |k|^3\right), \tag{2}$$

where c is the phase speed, and k the wavevector and H a dimensionless depth defined later. For all values of the depth H, the linear long wave speed $c = \sqrt{H}$ is a local maximum of c at $k = 0$. There is a global minimum of phase speed $c^*(H)$ at $k^*(H)$, at which $c = c_g \triangleq \omega'$. In infinite depth, $k^* = (1/3)^{1/4} \approx 0.76$ and $c^* \approx 1.32$ whereas in shallow water $k^* \sim H/\sqrt{6}$, $c^* =\sim \sqrt{H}(1 - \frac{1}{72}H^4)$. These features of the dispersion imply that two kinds of solitary waves might be expected in the system: shallow–water KP–type waves bifurcating from $k = 0$

(see [10]), and wave–packet type or "lump" solitary waves that may bifurcate from k^*. Solitary waves in this paper will be of the latter case. Typical physical values ([2] and [4]) for ice in two cases are: 1.6 m thick sheet, corresponding to $D \approx 1.6 \times 10^9 Nm$, over water 350 m deep at McMurdo Sound giving $H \approx 18$ and a minimal–speed wavelength of approximately 160 m; and 17 cm sheet, corresponding to $D \approx 2 \times 10^5 Nm$, over water 6.8 m deep in Lake Saroma, Hokkaido, giving $H \approx 3$ and a wavelength of approximately 20 m.

2. Governing equations and the BRDS system

Consider the motion of an irrotational, inviscid fluid bounded below by a horizontal bottom at $z = -H$ and above by a thin flexible massless sheet, which resists bending at $z = \eta(x, y, t)$. The free surface displacement and the velocity potential $\phi(x, y, z, t)$, then satisfy the problem

$$\phi_{xx} + \phi_{yy} + \phi_{zz} = 0 \quad -H < z < \epsilon\eta \tag{3}$$

$$\phi_z = 0 \quad \text{as } z = -H \tag{4}$$

$$\eta_t + \epsilon\left(\eta_x\phi_x + \eta_y\phi_y\right) = \phi_z \quad \text{at } z = \epsilon\eta \tag{5}$$

$$\phi_t + \frac{\epsilon}{2}\left(\phi_x^2 + \phi_y^2 + \phi_z^2\right) + \eta + \frac{\delta\mathbb{H}}{\delta\eta} = 0 \quad \text{at } z = \epsilon\eta. \tag{6}$$

These equations have been nondimensionalized using a lengthscale $(D/\rho g)^{1/4}$ and a timescale $\left(D/\rho g^5\right)^{1/8}$, where g is the acceleration due to gravity and ρ is the density of the liquid. $H \triangleq H_0\,(D/\rho g)^{-1/4}$ is a dimensionless depth parameter, where H_0 is the dimensional depth. The nonlinearity parameter ϵ is proportional to the wave–slope. $\mathbb{H}$ is the total energy due to bending defined in ((1)). The variational derivative $\frac{\delta\mathbb{H}}{\delta\eta}$ with respect to the surface displacement for the Cosserat model is

$$\begin{aligned}\frac{\delta\mathbb{H}_C}{\delta\eta} =& -2\partial_x[S(\eta_x\eta_{yy} - \eta_y\eta_{xy})] - 2\partial_y[S(\eta_y\eta_{xx} - \eta_x\eta_{xy})]\\ &+ \partial_{xx}[S(1+\eta_y^2)] - 2\partial_{xy}[S\eta_x\eta_y] + \partial_{yy}[S(1+\eta_x^2)]\\ &+ \frac{5}{2}\partial_x\left[S^2(1+|\nabla\eta|^2)^{3/2}\eta_x\right] + \frac{5}{2}\partial_y\left[S^2(1+|\nabla\eta|^2)^{3/2}\eta_y\right],\\ S =& \frac{(1+\eta_x^2)\eta_{yy} + (1+\eta_y^2)\eta_{xx} - 2\eta_x\eta_y\eta_{xy}}{(1+|\nabla\eta|^2)^{5/2}}.\end{aligned}$$

The present modulational theory, however, requires only nonlinear terms in the direction of propagation since bending in the transverse direction is much smaller. Hence, the expression above can be simplified to

$$\frac{\delta \mathbb{H}_C}{\delta \eta} = \Delta^2 \eta + \left\{ \partial_x^2 \left[\frac{\eta_{xx}}{(1+\eta_x^2)^{5/2}} \right] + \frac{5}{2} \partial_x \left[\frac{\eta_{xx}^2 \eta_x}{(1+\eta_x^2)^{7/2}} \right] - \partial_x^4 \eta \right\}, \tag{7}$$

and for the KL model, $\frac{\delta \mathbb{H}}{\delta \eta}$ is replaced by

$$\Delta^2 \eta + \left\{ \partial_x^2 \left[\frac{\eta_{xx}}{\left(1+\eta_x^2\right)^{3/2}} \right] - \partial_x^4 \eta \right\}.$$

The terms in brackets in the two expressions above are the nonlinear corrections for each model from the linear biharmonic model.

Modulational analysis is used extensively in water waves [16] and we only sketch the derivation of the BRDS system for small amplitude FG waves. On the free surface, $\phi(x, y, z, t) = \phi(x, y, \epsilon\eta, t)$, and, expanding this expression about $z = 0$,

$$\begin{aligned} \phi(x, y, z, t) = \phi(x, y, 0, t) + \epsilon\eta\phi_z(x, y, 0, t) + \tfrac{\epsilon^2\eta^2}{2}\phi_{zz}(x, y, 0, t) \\ + O(\epsilon^3). \end{aligned} \tag{8}$$

This allows rewriting the surface boundary conditions at $z = 0$ to cubic order as

$$\begin{aligned} \eta_t - \phi_z &= \epsilon \left(\eta\phi_{zz} - \phi_x\eta_x - \phi_y\eta_y \right) \\ &\quad + \epsilon^2 \left(\frac{1}{2}\eta^2\phi_{zzz} - \eta\eta_x\phi_{xz} - \eta\eta_y\phi_{yz} \right) \\ \phi_t + \left(1+\Delta^2\right)\eta &= \epsilon \left(-\eta\phi_{zt} - \frac{1}{2}\phi_x^2 - \frac{1}{2}\phi_y^2 - \frac{1}{2}\phi_z^2 \right) \\ &\quad + \epsilon^2 \Bigg(-\frac{1}{2}\eta^2\phi_{zzt} - \eta\phi_x\phi_{xz} - \eta\phi_y\phi_{yz} - \eta\phi_z\phi_{zz} \\ &\quad + \frac{5}{2}\eta_x^2\eta_{xxx} + \frac{5}{2}\eta_{xx}^3 + 10\eta_x\eta_{xx}\eta_{xxx} \Bigg). \end{aligned} \tag{9}$$

Consider now the propagation of a quasi–monochromatic wave whose slow dependence is comparable in both x– and y– directions, but whose fast oscillation is only in the propagation direction x. To derive the governing equation for the wave envelope, we introduce $X = \epsilon x$, $Y = \epsilon y$, $T = \epsilon t$, and $\tau = \epsilon^2 t$, and choose $e^{i(kx-\omega t)}$ as the carrier wave. One then seeks a solution of the form:

$$\phi = \phi_1(X - c_g T, Y, z, \tau, \Theta) + \epsilon\phi_2(X - c_g T, Y, z, \tau, \Theta) + \ldots + \text{c.c.} \tag{10}$$

$$\eta = A_1(X - c_g T, Y, \tau, \Theta) + \epsilon A_2(X - c_g T, Y, \tau, \Theta) + \ldots + \text{c.c.}, \tag{11}$$

where $\Theta \triangleq kx - \omega t$ and c.c. represents the complex conjugate. The ϕ_n and A_n may include all the harmonics up to n, thus

$$\phi_n = \phi_{n0}e^0 + \phi_{n1}e^{i\Theta} + \ldots + \phi_{nn}e^{in\Theta},$$

and similarly for A. The leading order quantities that will govern the evolution of the wave packet are $\phi_1 = \phi_{10}(X - c_g T, Y, \tau) + \phi_{11}(X - c_g T, Y, z, \tau)e^{i\Theta}$ and $A_1 = A_{11}(X - c_g T, Y, \tau)e^{i\Theta}$. ϕ_{10} represents a mean flow induced by the wave, and which is present at leading order in finite depth.

One then solves a sequence of problems at each order n and for each harmonic j:

$$\phi_{nj,zz} - (jk)^2\phi_{nj} = P_{nj}, \qquad \phi_{nj,z} = 0 \quad \text{at} \quad z = -H, \tag{12}$$

where P_{nj} is made up of known lower order terms. The solution to (12) has the form $\phi_{nj} = \varphi_{nj}(X - c_g T, Y, \tau)\cosh(jk(z + H))$ plus particular solutions arising from P_{nj}. This solution is substituted in the surface boundary conditions and one obtains equations of the form

$$(jk)\sinh(jkH)\varphi_{nj} + i(j\omega)A_{nj} = Q_{nj} \tag{13}$$

$$-i(j\omega)\cosh(jkH)\varphi_{nj} + \left(1 + (jk)^4\right)A_{nj} = R_{nj} \tag{14}$$

Q, R are also lower order terms. When $n = 1, j = 1$, $P = Q = R = 0$, a nontrivial solution implies the dispersion relation (2) for $c \triangleq \omega/k$.

At second and third orders ($n = 2, 3$), the equations are inhomogeneous and a considerable amount of algebra eventually results in solvability conditions at third order that yield the governing equations for the envelope A_{11} and the mean flow ϕ_{10}, henceforth denoted A and φ, respectively. They are found to satisfy the following BDRS system

$$\left(1 - H^{-1}c_g^2\right)\varphi_{XX} + \varphi_{YY} = \alpha\left(|A|^2\right)_X \tag{15}$$

$$i\,A_\tau + \frac{\omega''}{2}\,A_{XX} + \frac{c_g}{2k}\,A_{YY} + \beta A\varphi_X + \gamma|A|^2 A = 0. \tag{16}$$

The coefficients are given by,

$$\alpha = -\frac{1}{H}\left(\frac{\omega^2 c_g}{\sinh^2 kH} + \frac{2k(1+k^4)}{\omega}\right),$$

$$\beta = -\left[k + \frac{k^2(1+k^4)}{2\omega}\,\mathrm{sech}^2 kH\; c_g\right].$$

The only coefficient that depends on the elasticity model is γ. For the linear elasticity model, $\gamma = \gamma_L$, where

$$\gamma_L = \frac{\omega k^2}{4\tanh^2 kH} \frac{(1+k^4)\tanh^4 kH - 10(1+k^4)\tanh^2 kH + (9+69k^4)}{15k^4 - (1+k^4)\tanh^2 kH} + \frac{\omega k^2}{2}\left(\frac{1+k^4}{\sinh^2 kH \cosh^2 kH} - 4\right).$$

For the Cosserat or KL models, γ is modified by an additional term. That is,

$$\gamma = \gamma_L + \gamma_{C,K} \quad \text{with} \quad \gamma_C = \frac{5\omega k^6}{2(1+k^4)}, \quad \gamma_K = \frac{3\omega k^6}{4(1+k^4)}.$$

The remainder of this paper is devoted to solutions of the BRDS equations above and their consequences on FG wavepackets.

3. Results

3.1. Properties of the BRDS system at critical speed

The BRDS system ((16)) is valid for arbitrary $k > 0$, however, in this section we focus on the case $k = k^*$. Since $c_g^2 < H$, $\omega'' > 0$, and $c_g/2k > 0$ the system is of "elliptic–elliptic" type [18] as both the coefficients of φ_{XX} and φ_{YY} and of A_{XX} and A_{YY} are of the same sign. The behavior of the system then depends crucially on the sign of the parameters γ and

$$\mu = \frac{\alpha\beta}{1 - H^{-1}c_g^2} + \gamma.$$

The values of γ at μ at k^* are shown in Figure 1. The importance of these parameters can be seen by writing the BRDS system as the single nonlocal equation

$$iA_\tau + \frac{\omega''}{2}A_{XX} + \frac{c_g}{2k}A_{YY} - \frac{\alpha\beta}{1 - H^{-1}c_g^2}\tilde{\Delta}^{-1}[|A|^2]_{YY}A + \mu|A|^2A = 0, \qquad (17)$$

where $\tilde{\Delta} = \left(1 - H^{-1}c_g^2\right)\partial_{XX} + \partial_{YY}$. In infinite depth, the leading order effect of the mean flow vanishes since $\frac{\alpha\beta}{1-H^{-1}c_g^2} \sim 2k\omega H^{-1}$, and the evolution is governed by the two dimensional NLS equation

$$iA_\tau + \frac{\omega''}{2}A_{XX} + \frac{c_g}{2k}A_{YY} + \gamma|A|^2A = 0. \qquad (18)$$

This equation, is denoted *focussing* if $\gamma > 0$ and *defocussing* if $\gamma < 0$. For the FG problem, $\gamma < 0$ and thus the equation is defocussing in which case we can conclude that no small amplitude solitary waves exist in the full fluid

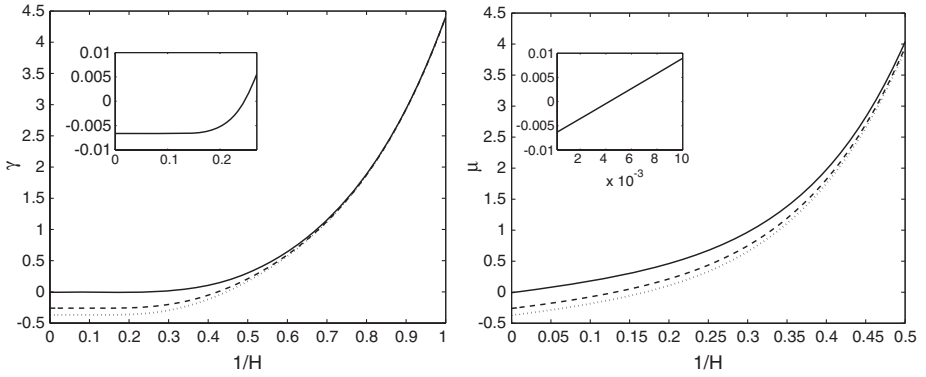

Figure 1. Left–hand side: Nonlinearity self–interaction parameter γ. Right–hand side: Nonlinearity parameter μ which includes mean flow effects. Three elasticity models are shown: Cosserat (solid line), Kirchoff–Love (dashed), and Linear (dotted). Details of the H large Cosserat case are also shown.

problem ((3)–(6)) in either one or two dimensions. Note, however, that in one dimension, *finite* amplitude solitary waves have been found in the full equations in [5] and [8].

For a two——dimensional fluid domain, the one dimensional NLS equation in *arbitrary* depth can be obtained from ((17))

$$i A_\tau + \frac{\omega''}{2} A_{XX} + \mu \left| A \right|^2 A = 0, \tag{19}$$

and was given by [4] in the KL case. In all three elasticity cases, in infinite depth, $\mu = \gamma < 0$ (i.e., defocussing or BF stable), but as H is decreased, the coefficient μ changes sign at critical values of the depth H^+, and the equation becomes focussing (BF unstable). In this case, wave packet solitary waves of the Euler equations can be expected. The mean flow provides an important contribution to this sign change (compare left and right panels of Figure 1). For the Cosserat model $H_C^+ \approx 233$, for the Linear model $H_L^+ \approx 5.91$ and for the KL model $H_{KL}^+ \approx 7.62$.

In arbitrary depth and in for a three–dimensional fluid domain, one can also write the BRDS system in a different form

$$i A_\tau + \frac{\omega''}{2} A_{XX} + \frac{c_g}{2k} A_{YY} + \alpha\beta \tilde{\Delta}^{-1} \left[\left| A \right|^2 \right]_{XX} A + \gamma \left| A \right|^2 A = 0. \tag{20}$$

The nonlocal term now describes the important focussing effect due to the mean–flow (since $\alpha\beta > 0$). From this form, [17] proved that $\mu > 0$ is a sufficient condition for the equation to have a localized ground state solitary wave. Henceforth we use this criterion to call the BRDS system focussing. (The fact $\mu > 0$ is also a necessary condition is evident from ((17)) where the nonlocal term is defocussing.) These solitary waves and their implication

for the full equations will de discussed below. Note that the system may be focussing even though the self–interaction coefficient, $\gamma < 0$. In fact this occurs for a range of depths $H^+ > H > H^-$ where H^- is the value of H at which γ changes sign. For the Cosserat model $H_C^- \approx 4.06$, for the Linear model $H_L^- \approx 2.24$ and for the KL model $H_{KL}^- \approx 2.36$. Therefore there is a wide regime where the induced mean flow is the mechanism for the BF instability.

3.2. Solitary waves

Our goal is to seek approximate localized steadily traveling solutions to the original problem ((3)–(6)). This corresponds to finding localized time harmonic solutions to the BRDS system since, when setting $A = e^{i\Omega\tau}\rho(X, Y)$, the leading order terms in ((10)–(11)) yield a traveling wave at speed c, where c is related to the amplitude of the wave by $c^* - c \sim \Omega a^2/4\rho(0,0)^2$, where a is half the peak to trough wave–height. Ω may be set to 1 by a scaling $\rho \to \Omega^{\frac{1}{2}}\rho$ (together with scalings in X and Y). The steady BRDS system in the nonlocal form of (20) then becomes

$$-\rho + \frac{\omega''}{2}\rho_{XX} + \frac{c_g}{2k}\rho_{YY} + \theta\alpha\beta\tilde{\Delta}^{-1}\left[\rho^2\right]_{XX}\rho + \gamma\rho^3 = 0, \tag{21}$$

with $\theta = 1$. The arbitrary parameter $\theta \in [0, 1]$ was introduced in the equation above to simplify the numerical solution of the problem, which proceeds in two steps. First, setting $\theta = 0$ the problem can be reduced by rescaling ρ, X, and Y for $\gamma > 0$ to the cubic NLS equation

$$-\rho + \rho_{XX} + \rho_{YY} + \rho^3 = 0, \tag{22}$$

for which axisymmetric solutions with $r = (X^2 + Y^2)^{1/2}$ satisfying

$$\frac{d^2\rho}{dr^2} + \frac{1}{r}\frac{d\rho}{dr} - \rho + \rho^3 = 0, \quad \frac{d\rho}{dr} = 0 \text{ at } r = 0, \quad \rho \to 0 \text{ as } r \to \infty,$$

can be sought. This equation has countably many solutions indexed by the number of zeros of $\rho(r)$. We focus only on the ground state solution. Second, the axisymmetric scaling is undone and the nonlocal term in ((21)) is included by using a numerical continuation in θ up to $\theta = 1$. This results in a solution to the full problem. The amplitude of the ground state (measured as $\rho(0, 0)$) is shown in Figure 2. The nonlinear speed correction and the typical length scale of the solitary wave (envelope) is

$$c^* - c \sim \left(\frac{a}{2\rho(0,0)}\right)^2, \qquad L_x, L_y \sim \left(\frac{a}{2\rho(0,0)}\right)^{-1}.$$

In Figure 2 note that as $H \uparrow H^+$ (μ approaches zero), $\rho(0, 0)$ diverges, and thus for fixed wave amplitude a the solitary packets become more spread and less nonlinear (the speed correction decreases). Typical solitary wave and

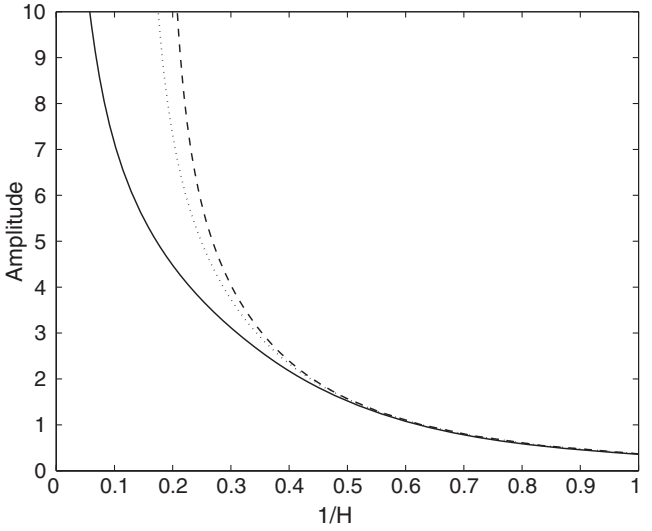

Figure 2. Ground state amplitude $\rho(0,0)$ as a function of inverse depth for the three elastic models: Cosserat (solid line), Kirchoff–Love (dotted), and Linear (dashed).

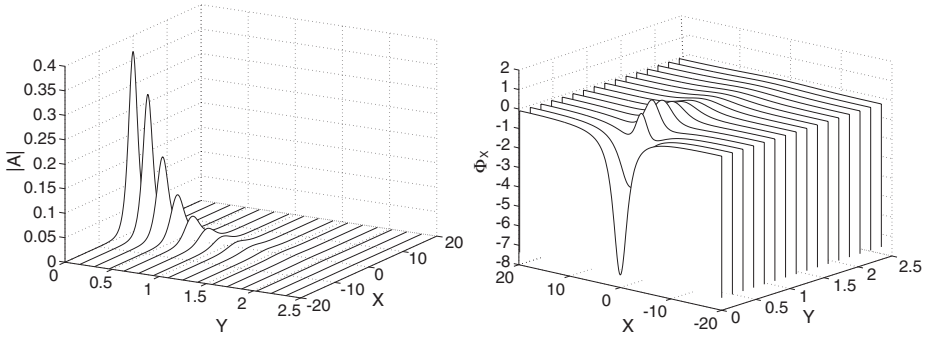

Figure 3. Shallower water, Kirchoff–Love model, $H = 1$. Left–hand side: Wavepacket amplitude. Right–hand side: Mean flow. Note that Φ_X is shown. The physical mean flow is one order smaller since $\Phi_x = \epsilon \Phi_X$.

mean–flow profiles are shown in Figures 3 and 4 for a shallower and deeper case, respectively. In the deeper case, the surface wave envelopes solutions become more anisotropic and have a distinctive X–shape as the depth increases. (The X–shape in the surface displacement envelope should not be confused with the X–shape of the mean flow in dromion solutions of [11].) The figures are shown for the KL model, but other models are similar.

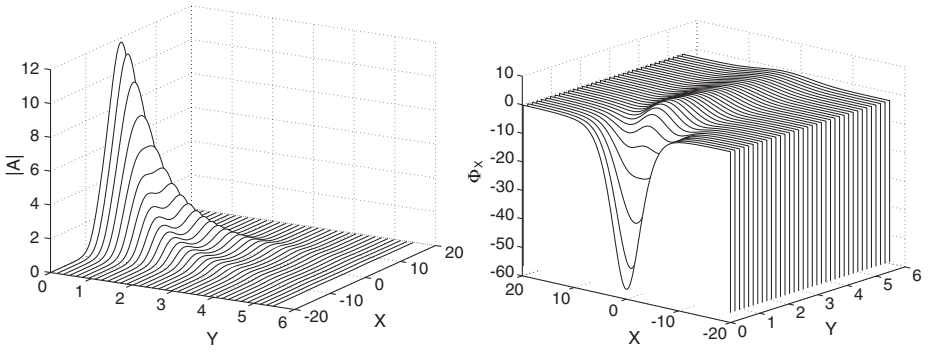

Figure 4. Deeper water, KL model, $H = 6$. Left–hand side: Wavepacket amplitude. Right–hand side: Mean flow.

3.3. Stability

The solutions found here are unstable (within the BRDS equations) from considerations similar to those that lead to the same conclusions for the focussing NLS equations. This result can be seen through a virial argument given in [18]. In the current context, the Hamiltonian for BRDS is

$$\mathcal{H} = \int \frac{\omega''}{2}|A_X|^2 + \frac{c_g}{2k}|A_Y|^2 - \frac{1}{2}\left(\gamma|A|^4 + \alpha\beta|A|^2\tilde{\Delta}^{-1}\left[|A|^2\right]_{XX}\right)dXdY.$$

The BRDS evolution, in addition, preserves $M_0 = \int |A|^2$. The variance $M_2(t) = \int (\frac{2}{\omega''}X^2 + \frac{2k}{c_g}Y^2)|A|^2$ evolves with $M_2'' = 8\mathcal{H}$. The ground correspond to $\mathcal{H} = 0$, and therefore perturbations resulting in $\mathcal{H} < 0$ will force $M_2 \geq 0$ to zero in finite time, collapsing the solution to a point. Conversely an $\mathcal{H} > 0$ perturbation will lead to a dispersive spreading of the wave. This instability however does not rule out stable solitary wave solutions to the original fluid problem. An analogy can be drawn to the instability of infinitely deep CG waves explained in [19]. There the envelope equation is the 2D focussing NLS, also with unstable localized solutions. However, nonlinear computations with the full equations revealed that (i) the branch of solutions corresponding to NLS ground states becomes stable at finite amplitude and (ii) in time dependent dynamics, the focussing collapse instability is arrested by nonlinearity at large amplitudes and results in localized traveling solitary or breather–type solutions. Similar computations on the primitive equations for the FG case are beyond the scope of this paper, but it is plausible that similar behavior takes place.

3.4. Dynamics away from minimal speed

The BRDS equations, of course, also govern the dynamics of *unsteady* wave packets when $k \neq k^*$. The stability conclusions of the previous section apply

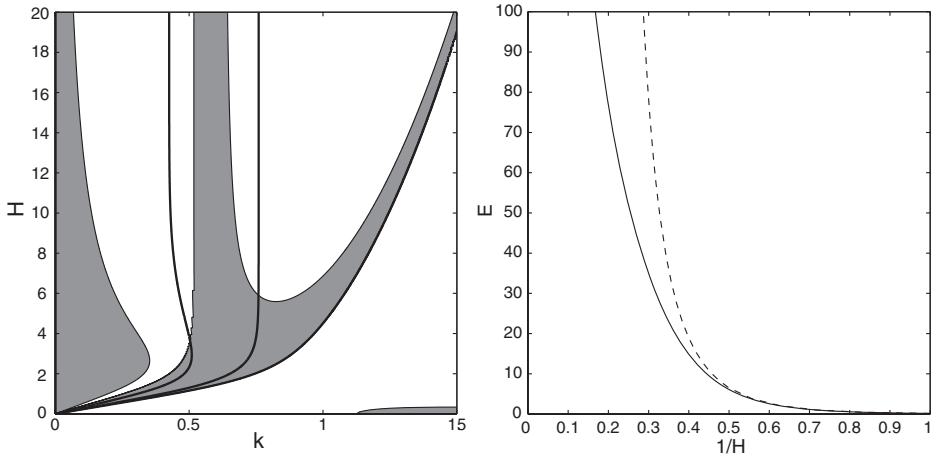

Figure 5. Left–hand side: Parameter regimes of the BRDS equation for the linear model. The shaded areas correspond to $\mu > 0$ (focussing). The three bold curves are, from left to right, $k^-(H)$, $k^*(H)$, and $k^+(H)$. The shaded region between $k^-(H)$ and $k^+(H)$ corresponds to the focussing elliptic–elliptic BRDS regime. The intersection of $k^*(H)$ with the boundary of the shaded region defines H_L^+. Right–hand side: Physical energy of ground states in units of D for the Cosserat model (solid) and linear model (dashed).

whenever the system is of focussing "elliptic–elliptic" type. In the current setting, it requires that the carrier wave be within a range of wave numbers depending on H. The requirements for this are: (i) $\omega'' > 0$ which is satisfied for all $k^-(H) < k < \infty$ with $k^- \to 0$ as $H \to 0$ and $k^- \approx 0.426$ as $H \to \infty$; (ii) $c_g^2 < H$ which is satisfied for all $0 < k < k^+(H)$ with $k^+(H) \to 0$ as $H \to 0$ and $k^+(H) \sim 0.54H^{1/3}$ as $H \to \infty$; (iii) $\mu > 0$. Of course, the interval $[k^-, k^+]$ always includes k^* and in practice, these conditions gives a broad range of wave numbers where the theory applies (see Figure 5). The figure is shown for the linear model, and for the Cosserat model, the focussing region extends into considerably deeper water with $H_C^+ \approx 233$. Within this region, wavepackets with $\mathcal{H} < 0$ will focus. The significance of this condition can be seen by considering the ground state solutions to ((21)) as the minimizer of the leading order physical energy of the wavepacket $E = (1 + k^4) \int \rho^2 dX dY$ subject to the constraint that $\mathcal{H}$ is fixed. Thus, they provide a lower bound for the physical energy required for an arbitrary wavepacket disturbance to undergo focussing. The physical energy of the minimizers at k^* for the linear and Cosserat models (the only two models for which we have an expression for the energy) are shown in Figure 5. Since the threshold energy decreases with depth, the triggering of a focussing instability due to shoaling seems particularly likely and may give an alternate explanation for the observations of [12]. In the left panel of Figure 5 the dromion solutions of [11] occur in the

unshaded parameter regime to the right of the curve $k^+(H)$, although only solutions near $H = 0$ were considered.

4. Conclusions

Two dimensional modulations of quasi–monochromatic FG waves were considered and shown to have complex behavior. Based on our analysis, small amplitude fully localized solitary waves exist up to a critical depth; in deeper water we conjecture that only *finite* amplitude localized waves exist. Three elasticity models were compared and found to have qualitatively similar results but substantial quantitative differences. We consider the KL model to be somewhat suspect since we cannot formulate it in conservation form. Nonlinearities in the elasticity term *decrease* the nonlinear frequency correction in infinite depth where all cases are Benjamin–Feir stable. In finite depth, however, mean flow effects trigger a modulational instability. For the energy conserving nonlinear Cosserat model this happens in relatively deep water ($H \approx 233$). The modulational instability can be violent, with a focussing singularity occurring in finite time. While larger amplitude solutions should be studied with fully nonlinear models, the initial stages of the Energy focussing mechanism could be a factor in the breakup of continuous ice sheets under forcing from open ocean waves.

Acknowledgments

This work was supported by EPSRC, under grant no. EP/J019321/1, and by the Division of Mathematical Sciences at the National Science Foundation, under grant no. DMS–0908077 and by a Royal Society Wolfson Research Merit award.

References

1. V.A. Squire, Of ocean waves and sea–ice revisited, *Cold Reg. Sci. Tech.*, 49:110–133 (2007).
2. V.A. Squire, R.J. Hosking, A.D. Kerr, and P.J. Langhorne, Moving loads on ice plates, *Solid Mechanics and its Applications*, Kluwer Academic Publishers, The Netherlands, (1996).
3. P.I. Plotnikov and J.F. Toland, Modelling nonlinear hydroelastic waves, *Phil. Tran. R. Soc. A*, 369:2942–2956 (2011).
4. E. Parau and F. Dias, Nonlinear effects in the response of a floating ice plate to a moving load, *J. Fluid Mech*., 460:281–305 (2002).

5. P.A. Milewski, J.–M. Vanden–Broeck and Z. Wang, Hydroelastic solitary waves in deep water, *J. Fluid Mech*., 679:628–640 (2011).
6. L.K. Forbes, Surface waves of large amplitude beneath an elastic sheet. Part 1. High–order series solution, *J. Fluid Mech*., 169:409–428 (1986).
7. J.–M. Vanden–Broeck and E. Parau, Two–dimensional generalised solitary waves and periodic waves under an ice sheet, *Phil. Trans. R. Soc. A*, 369:2957–2972 (2011).
8. P. Guyenne and E. Parau, Computations of fully nonlinear hydroelastic solitary waves on deep water, *J. Fluid Mech*., 713:307–329 (2012).
9. E. Parau and J.–M. Vanden–Broeck, Three–dimensional waves beneath an ice sheet due to a steadily moving pressure, *Phil. Trans. R. Soc. A*, 369:2973–2988 (2011).
10. M. Haragus–Courcelle and A. Il'ichev, Three–dimensional solitary waves in the presence of additional surface effects, *Eur. J. Mech. B/Fluids*, 17:739–768 (1998).
11. M.–R. Alam, Dromions of Flexural Gravity Waves, *J. Fluid Mech*., in press (2013).
12. A.K. Liu and E. Mollo–Christensen, Wave propagation in a solid ice pack, *J. Phys. Oceanogr*., 18:1702–1712 (1988).
13. D.J. Benney and G. Roskes, Wave instabilities, *Stud. Appl. Math.*, 48:377–385 (1969).
14. A. Davey and K. Stewartson On three–dimensional packets of the surface waves, *Proc. Royal Soc. Lond. A*, 338(1613):101–110 (1974).
15. B. Kim and T.R. Akylas, On gravity–capillary lumps, *J. Fluid Mech*., 540:337–351 (2005).
16. M.J. Ablowitz and H. Segur, On the evolution of packets of water waves, *J. Fluid Mech*., 92:691–715 (1979).
17. R. Cipolatti, On the existence of standing waves for the Davey–Stewartson system, *Comm. Part. Diff. Eqn*., 17:967–988 (1992).
18. C. Sulem and P.L. Sulem, The nonlinear Schrördinger equation: self–focusing and wave collapse, *Applied Mathematical Sciences*, Vol. 139, Springer-Verlag, New York, (1999).
19. Z. Wang and P.A. Milewski, Dynamics of gravity–capillary solitary waves in deep water, *J. Fluid Mech*., 708:480–501 (2012).

University of Bath
University of Wisconsin–Madison

(Received January 25, 2013)